Challenging the rate-state asperity model: Afterslip following the 2011 M9 Tohoku-oki, Japan, earthquake

Kaj M. Johnson,[1] Jun'ichi Fukuda,[2] and Paul Segall[3]

Received 28 June 2012; revised 5 September 2012; accepted 9 September 2012; published 17 October 2012.

[1] Prior to the 2011 M9 Tohoku-oki earthquake, subduction at the Japan Trench was characterized by M7-8 earthquakes, sometimes rupturing the same source regions (seismic asperities), followed by extensive afterslip detected by GPS measurements. A physically-based model consisting of velocity-weakening asperities surrounded by aseismic creep on velocity-strengthening regions (the 'rate-state asperity model') became the prevailing conceptual model for earthquakes in this region. Theory and numerical simulation indicates that velocity-weakening areas do not exhibit sustained afterslip, while velocity-strengthening regions do not accumulate stress interseismically. Here we demonstrate that the rate-state asperity model is contradicted by models of postseismic deformation following the Tohoku-oki earthquake: afterslip in the first eight months either occurred on historical seismic asperities or stress accumulated in regions surrounding the asperities. Unsmoothed inversions of cumulative 8-month postseismic GPS displacements that restrict afterslip to areas outside of historical ruptures cannot fit the data without afterslip exceeding the slip that fully relaxes the coseismic stress change. In contrast, similarly constrained inversions allowing slip within historical ruptures can satisfactorily fit the postseismic displacements. These results require a modification of the rate-state asperity model and raise new questions about physical processes and properties of the subduction interface. **Citation:** Johnson, K. M., J. Fukuda, and P. Segall (2012), Challenging the rate-state asperity model: Afterslip following the 2011 M9 Tohoku-oki, Japan, earthquake, *Geophys. Res. Lett.*, *39*, L20302, doi:10.1029/2012GL052901.

1. Introduction

[2] The asperity model for the NE Japan subduction zone, consisting of a number of rupture patches (asperities) that exhibit repeated earthquakes of various sizes surrounded by creeping fault areas, is a widely-held conceptual model [*Lay and Kanamori*, 1980] supported by a number of observations. Before the 2011 M9 Tohoku-oki megathrust event, slip on the plate interface was characterized by a number of M7-8 ruptures with evidence of repeated rupture of the same fault patches [*Yamanaka and Kikuchi*, 2004; *Iinuma protect et al.*, 2011]. Post-seismic GPS displacements are interpreted to show unusually large afterslip following these events [e.g., *Suito et al.*, 2011; *Yagi et al.*, 2003], often surrounding the coseismic ruptures [e.g., *Yagi et al.*, 2003; *Miyazaki et al.*, 2004]. In addition, *Igarashi et al.* [2003] and *Uchida and Matsuzawa* [2011] show that small repeating earthquakes, which are commonly interpreted to occur on stuck patches in an otherwise creeping fault, occur over large areas of the plate interface that are inferred to exhibit low coupling based on geodetic inversions. In contrast, few repeating earthquakes occur in areas inferred to be locked.

[3] A mechanical interpretation of the asperity model cast in terms of the rate-state friction has been proposed by various authors [e.g., *Scholz*, 1990; *Boatwright and Cocco*, 1996; *Igarashi et al.*, 2003]. This model consists of earthquakes occurring on velocity-weakening asperities surrounded by creep on velocity-strengthening regions. A consequence of this 'rate-state asperity model' is that parts of the fault that are known to have ruptured in past earthquakes (i.e., seismic asperities) are unlikely to slide stably in response to an external stress [*Rice and Gu*, 1983] and would not display measurable amounts of stable afterslip following dynamic rupture [*Segall*, 2010, p. 362].

[4] Coseismic slip during the 2011 M9 Tohoku-oki earthquake appears to partly overlap previously identified asperities as shown in Figure 1 [*Iinuma et al.*, 2011; A. Hooper et al., Importance of horizontal seafloor motion on tsunami height for the Mw = 9.0 Tohoku-oki earthquake, submitted to *Earth and Planetary Science Letters*, 2012] and it has been suggested that the M9 earthquake may have ruptured through velocity-strengthening regions surrounding these asperities [e.g., *Shibazaki et al.*, 2011]. It also appears from slip inversions of postseismic GPS displacements [e.g., *Ozawa et al.*, 2011, 2012] that afterslip following the Tohoku-oki earthquake may overlap historical rupture zones, contradicting the rate-state asperity model. Most afterslip inversions, however, are heavily smoothed so it is not clear whether slip in the seismic asperities is required to fit the data. In this study, we test the rate-state asperity model using unsmoothed inversions of 8-month cumulative postseismic GPS displacements after the Tohoku-oki earthquake to test whether slip is indeed required in the previously identified asperities.

2. Method

[5] To test the rate-state asperity model, we compare slip inversions in which afterslip is not allowed within the historical earthquake asperities in Figure 1 (called 'no-asperity-slip inversions') with inversions that allow afterslip within the asperities (called 'asperity-slip inversions'). We invert eight months of cumulative postseismic displacements

[1]Department of Geological Sciences, Indiana University, Bloomington, Indiana, USA.
[2]Earthquake Research Institute, University of Tokyo, Tokyo, Japan.
[3]Department of Geophysics, Stanford University, Stanford, California, USA.

Corresponding author: K. M. Johnson, Department of Geological Sciences, Indiana University, Bloomington, IN 47405, USA. (kajjohns@indiana.edu)

0094-8276/12/2012GL052901

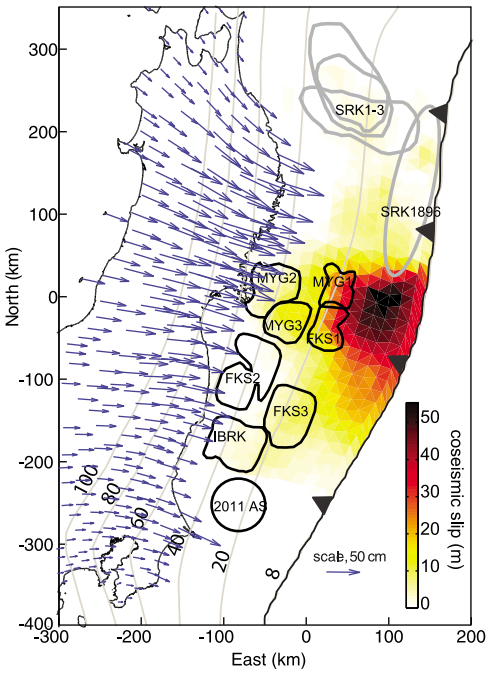

Figure 1. Coseismic slip during the 2011 M 9 Tohoku-oki earthquake (A. Hooper et al., submitted manuscript, 2012), locations and approximate spatial extent of historical earthquake ruptures, and 8-month cumulative postseismic displacements from GPS data. SRK 1896 – 1896 M8.5, SRK1-3 – 1901 M7.4, 1931 M7.6, 1933 M7.6, MYG1 – 1981 M7.1, MYG2 – 1978 M7.4, 2005 M7.2, MYG3 – 1936 M7.4, FKS1 – 2003 M6.8, FKS2 – 1938 M7.3, FKS3 – 1938 M7.5, IBRK – 1938 M7.0, 2011 AS – 2011 M7.7 aftershock. Asperity locations taken from *Yamanaka and Kikuchi* [2004] and *Shibazaki et al.* [2011].

computed from GPS data shown in Figure 1. We use GPS data from 291 stations of the Japanese continuous GPS network GEONET in northeastern Japan from March 11 to November 6, 2011. The GPS data are analyzed using the GIPSY-OASIS II software [*Zumberge et al.*, 1997]. We use a single-receiver bias-fixed precise point positioning strategy [*Bertiger et al.*, 2010] to estimate daily site coordinates in a North American plate-fixed reference frame based on NNR-NUVEL1A [*Argus and Gordon*, 1991; *DeMets et al.*, 1994]. We estimate and remove aftershock static offsets with a Kalman filter/smoother by modeling GPS coordinate time series as the sum of aseismic displacements, coseismic offsets, reference frame errors, and measurement errors [*Miyazaki et al.*, 2006]. Temporal variations of aseismic displacements and reference frame errors are modeled as integrated random walk and white noise processes, respectively, while coseismic offsets are modeled with Heaviside step functions, and measurement errors are assumed to follow a Gaussian distribution. We estimate cumulative postseismic displacements by subtracting the position at the first epoch of the time series from the mean of the last 14 epochs. Formal uncertainties are propagated to obtain uncertainties in the cumulative displacements.

[6] We adopt the subduction interface geometry from *Miyazaki et al.* [2011]. The interface is discretized into triangular dislocation elements in an elastic plate overlying a linear, Maxwell, viscoelastic half-space. We find that including viscoelastic flow at depth improves the fit to the GPS data and nearly removes a systematic misfit of 5–10 cm in the horizontal and vertical displacements resulting from elastic half-space inversions (see Figure S1 of the auxiliary material for more details), however conclusions about slip within asperities does not depend on whether or not viscoelastic flow is modeled.[1] In all inversions presented here, we include the influence of flow below 60 km depth with a half-space relaxation time of 2.5 years (viscosity of approximately 10^{18} Pa s). Flow is induced by imposing the coseismic slip distribution shown in Figure 1; for simplicity, we do not model the postseismic flow in response to afterslip (we invert for afterslip using an elastic half-space model).

[7] There are two important consequences of the simple asperity model: 1. velocity-weakening regions do not exhibit sustained afterslip [e.g., *Segall*, 2010; *Rice and Gu*, 1983], and 2. velocity-strengthening regions creep at constant stress interseismically, that is without stress accumulation [e.g., *Hetland et al.*, 2010, Figure 13], but rapidly creep postseismically to relax imposed coseismic stresses. Because stress does not accumulate interseismically on creeping parts of the fault, the maximum afterslip is that which fully relaxes the coseismic stress change. If the simple asperity model is correct, we should be able to fit the 8-month postseismic displacements in a no-asperity-slip inversion with slip nowhere exceeding the fully relaxed afterslip. In this study, fully relaxed afterslip is computed from the coseismic slip distribution of (A. Hooper et al., submitted manuscript, 2012) using a boundary element method (Figure 2b) with coseismic slip less than 10m set to zero to maximize the coseismic shear stress change down-dip of the rupture. Coseismic slip due to the M7.7 aftershock (2011 SA in Figure 1) is modeled following *Simons et al.* [2011]. We solve for the slip that completely releases the coseismic shear stress on the part of the fault that experienced a positive shear stress change.

[8] The underdetermined geodetic slip inverse problem is commonly regularized to seek smooth slip distributions [e.g., *Du et al.*, 1992]. To avoid effects of *a priori* regularization, we bound the slip, but otherwise apply no regularization [e.g., *Murray and Segall*, 2002; *Simons et al.*, 2011]. Let $\mathbf{s}^s = (s_1^s, s_2^s, \ldots, s_N^s)$ and $\mathbf{s}^d = (s_1^d, s_2^d, \ldots, s_N^d)$ be vectors of strike- and dip-slip components of afterslip on N elements, and define the vector $\mathbf{s} = (\mathbf{s}^s, \mathbf{s}^d)$. We apply non-negativity constraints on $\mathbf{s}^d$ (slip is required to be reverse sense). Let $\mathbf{d}$ be a vector of data and $\mathbf{G}$ be a matrix of half space Green's functions. We minimize $\|\mathbf{d} - \mathbf{Gs}\|_2$ subject to $s_i^d > 0$ for $i = 1, \ldots, N$, and refer to this as a 'non-negative' inversion. We define vectors of strike- and dip-components of fully relaxed afterslip, $\mathbf{r}^s = (r_1^s, r_2^s, \ldots, r_N^s)$ and $\mathbf{r}^d = (r_1^d, r_2^d, \ldots, r_N^d)$. For inversions bounded by fully relaxed afterslip, we minimize $\|\mathbf{d} - \mathbf{Gs}\|_2$ subject to $s_i^d > 0$ and $|s_i^s| \le \max(1m, r_i^s)$ and $|s_i^d| \le \max(1m, r_i^d)$ for $i = 1, \ldots, N$ (where all slip components are in meters). To be conservative, we have adopted a minimum upper bound of 1 m slip to allow relatively small deviations from relaxed bounds in areas of low fully relaxed slip.

[9] For the no-asperity-slip inversions, we represent each asperity with circular patches of radius 20 km, which is conservative for the purpose of testing the asperity model in the

[1] Auxiliary materials are available in the HTML. doi:10.1029/2012GL052901.

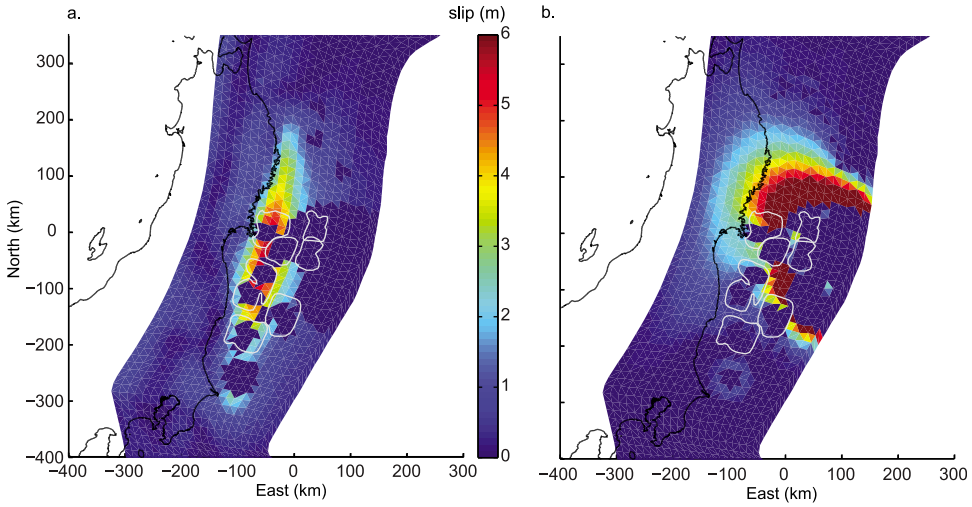

Figure 2. (a) Non-negative, no-asperity-slip inversion with no upper bounds on slip. See auxiliary materials for version with slip vectors shown. (b) Fully relaxed afterslip without slip in asperities. Color shows total slip in Figures 2a nd 2b. Colorscale is saturated at 6 m (maximum slip in Figure 2a). Gray lines show outlines of asperities denoted in Figure 1.

sense that these are smaller than the actual rupture areas in Figure 1.

3. Results

[10] Figure 2a shows the non-negative, no-asperity-slip inversion without upper bounds on slip. The fit to the data is very good with a normalized chi-square of $\chi_n^2 = 0.79$ (normalized chi-square is defined here as the sum of squared weighted residuals divided by number of observations). However, slip in some places greatly exceeds the fully relaxed bound shown in Figure 2b. Therefore, while it is indeed possible to fit the data with a no-asperity-slip model, the amount of afterslip exceeds plausible physical bounds in places. Figure 3a shows the no-asperity-slip inversion with fully relaxed bounds (as in Figure 2b). The fit to the horizontal GPS displacements (Figure 3b) is relatively poor ($\chi_n^2 = 1.88$). In particular, horizontal displacements in the eastern half of Honshu are systematically underestimated, especially in the vicinity of asperities, with misfits up to 20 cm.

[11] Figure 4 shows that the asperity-slip inversion with fully relaxed bounds does fit the data well ($\chi_n^2 = 0.6$). This inversion clearly requires non-negligible amounts of afterslip on historical rupture asperities.

4. Discussion and Conclusions

[12] Velocity-weakening regions are not expected to exhibit sustained afterslip. *Rice and Gu* [1983] showed that a single-degree-of-freedom spring-slider with velocity-weakening friction can display a stable transient response to an external stress perturbation, but this can happen only within a very narrow range of stress changes and initial

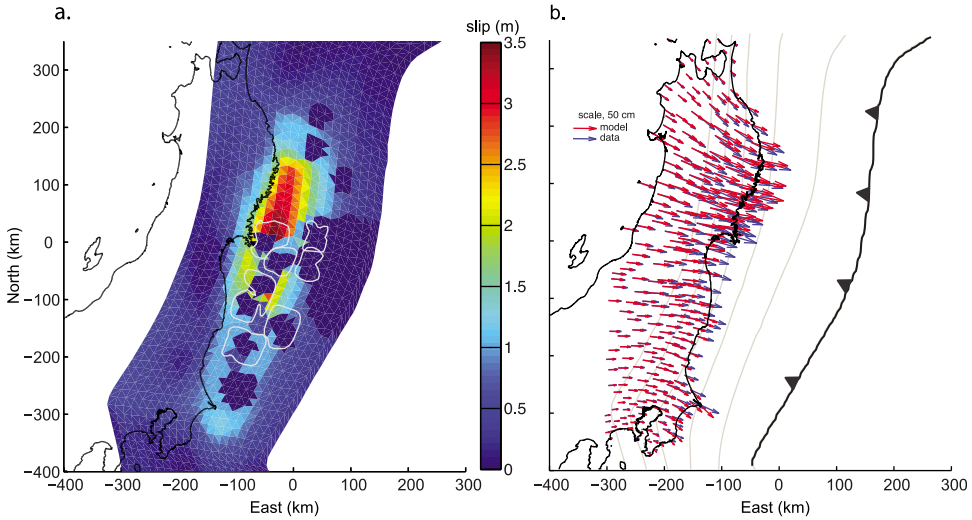

Figure 3. (a) No-asperity-slip inversion bounded by fully relaxed afterslip. Note color scale is different from Figure 2. Gray lines show outlines of asperities denoted in Figure 1. Color shows total slip. See auxiliary materials for version with slip vectors shown. (b) Fit to horizontal GPS displacements.

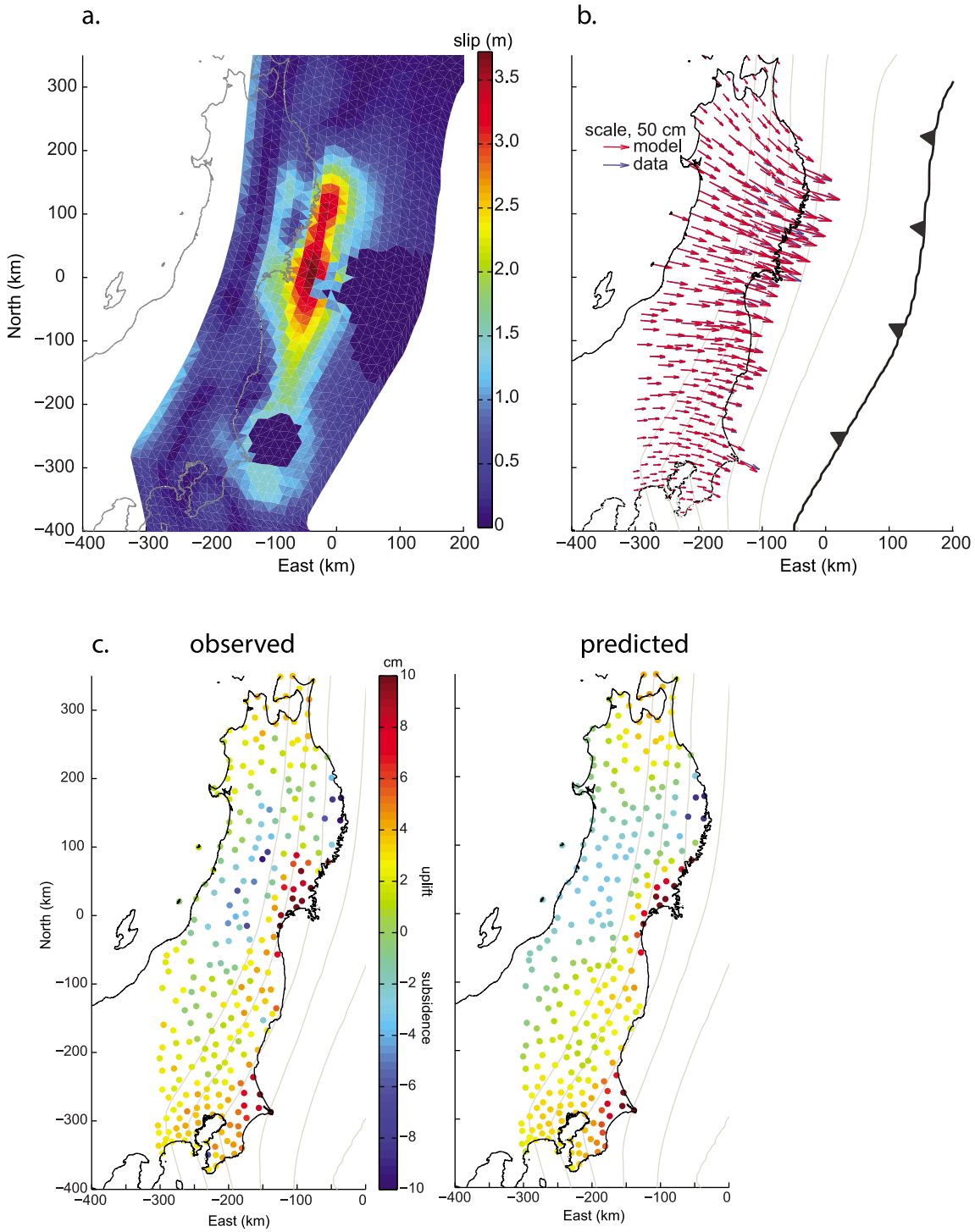

Figure 4. (a) Asperity-slip inversion bounded by fully relaxed afterslip. Color shows total slip. See auxiliary materials for version with slip vectors shown. (b) Fit to horizontal GPS displacements. (c) Fit to vertical GPS displacements.

conditions. Most stress perturbations lead either to no transient or unstable slip. It is also unlikely that velocity-weakening regions that ruptured during the 2011 M9 event would continue to slide throughout the postseismic period. *Rubin and Ampuero* [2005] (see also *Segall* [2010]) showed that the deceleration phase of slip on a velocity-weakening patch is short (hours to days) for reasonable values of rate-state friction parameters and the amount of slip is below the detection threshold of GPS measurements.

[13] We have shown that the simple rate-state asperity model is inconsistent with afterslip following the M9 Tohoku-oki earthquake. To fit the observed 8-month cumulative postseismic displacements, either afterslip is required within historical earthquake asperities or afterslip surrounding asperities must exceed the fully relaxed limit. This is inconsistent with a simple model consisting of velocity-weakening patches obeying simple rate-state friction surrounded by a velocity-strengthening interface.

[14] It is beyond the scope of this paper to explore possible mechanisms for afterslip on velocity-weakening asperities, stress-accumulation in 'non-asperity' regions, or other possible explanations for the observations. One possibility is that coseismic slip, and consequently fully relaxed afterslip, in the vicinity of asperities is more heterogeneous than can be inferred from standard slip inversions (see Figure S5 of the auxiliary material). Alternatively, the idealized model may be lacking in some important aspects and perhaps other physical mechanisms, in addition to rate-state friction, are engaged during slip. Future research will focus on identifying plausible mechanisms for generating afterslip on nominally velocity-weakening asperities or accumulating stress in velocity-strengthening regions.

[15] **Acknowledgments.** We thank the Geospatial Information Authority of Japan for the GPS data access.

[16] The Editor thanks two anonymous reviewers for their assistance in evaluating this paper.

References

Argus, D. F., and R. G. Gordon (1991), No-net-rotation model of current plate velocities incorporating plate motion model nuvel-1, *Geophys. Res. Lett.*, *18*(11), 2039–2042, doi:10.1029/91GL01532.

Bertiger, W., S. Desai, B. Haines, N. Harvey, A. Moore, S. Owen, and J. Weiss (2010), Single receiver phase ambiguity resolution with gps data, *J. Geod.*, *84*, 327–337.

Boatwright, J., and M. Cocco (1996), Frictional constraints on crustal faulting, *J. Geophys. Res.*, *101*, 13,895–13,909.

DeMets, C., R. G. Gordon, D. F. Argus, and S. Stein (1994), Effect of recent revisions to the geomagnetic reversal time scale on estimates of current plate motions, *Geophys. Res. Lett.*, *21*(20), 2191–2194, doi:10.1029/94GL02118.

Du, Y., A. Aydin, and P. Segall (1992), Comparison of various inversion techniques as applied to the determination of a geophysical deformation model for the 1983 borah peak earthquake, *Bull. Seismol. Soc. Am.*, *82*, 1840–1866.

Hetland, E. A., M. Simons, and E. Dunham (2010), Post-seismic and interseismic fault creep I: Model description, *Geophys. J. Int.*, *181*, 81–98, doi:10.1111/j.1365–246X.2010.04522.x.

Igarashi, T., T. Matsuzawa, and A. Hasegawa (2003), Repeating earthquakes and interplate aseismic slip in the northeastern japan subduction zone, *J. Geophys. Res.*, *108*(B5), 2249, doi:10.1029/2002JB001920.

Iinuma, T., M. Ohzono, Y. Ohta, and S. Miura (2011), Coseismic slip distribution of the 2011 off the pacific coast of tohoku earthquake (M 9.0) estimated based on GPS data: Was the asperity in Miyagi-oki ruptured?, *Earth Planets Space*, *63*, 643–648.

Lay, T., and H. Kanamori (1980), An apserity model of large earthquake sequences, in *Earthquake Prediction, An International Review*, edited by D. Simpson and P. Richards, pp. 579–592, AGU, Washington, D. C.

Miyazaki, S., P. Segall, J. Fukuda, and T. Kato (2004), Space time distribution of afterslip following the 2003 Tokachi-oki earthquake: Implications for variations in fault zone frictional properties, *Geophys. Res. Lett.*, *31*, L06623, doi:10.1029/2003GL019410.

Miyazaki, S., P. Segall, J. J. McGuire, T. Kato, and Y. Hatanaka (2006), Spatial and temporal evolution of stress and slip rate during the 2000 Tokai slow earthquake, *J. Geophys. Res.*, *111*, B03409, doi:10.1029/2004JB003426.

Miyazaki, S., J. J. McGuire, and P. Segall (2011), Seismic and aseismic fault slip before and during the 2011 off the Pacific coast of Tohoku earthquake, *Earth Planets Space*, *63*, 637–642, doi:10.5047/eps.2011.07.001.

Murray, J., and P. Segall (2002), Testing time-predictable earthquake recurrence by direct measurement of strain accumulation and release, *Nature*, *419*, 287–291.

Ozawa, S., T. Nishimura, H. Suito, T. Kobayashi, M. Tobita, and T. Imakiire (2011), Coseismic and postseismic slip of the 2011 magnitude-9 Tohoku-oki earthquake, *Nature*, *475*, 373–376, doi:10.1038/nature10227.

Ozawa, S., T. Nishimura, H. Munekane, H. Suito, T. Kobayashi, M. Tobita, and T. Imakiire (2012), Preceding, coseismic, and postseismic slips of the 2011 Tohoku earthquake, Japan, *J. Geophys. Res.*, *117*, B07404, doi:10.1029/2011JB009120.

Rice, J. R., and J.-C. Gu (1983), Earthquake aftereffects and triggered seismic phenomena, *Pure Appl. Geophys.*, *121*, 187–219.

Rubin, A. M., and J.-P. Ampuero (2005), Earthquake nucleation on (aging) rate and state faults, *J. Geophys. Res.*, *110*, B11312, doi:10.1029/2005JB003686.

Scholz, C. H. (1990), *The Mechanics of Earthquakes and Faulting*, Cambridge Univ. Press, New York.

Segall, P. (2010), *Earthquake and Volcano Deformation*, Princeton Univ. Press, Princeton, N. J.

Shibazaki, B., T. Matsuzawa, A. Tsutsumi, K. Ujiie, A. Hasegawa, and Y. Ito (2011), 3D modeling of the cycle of a great Tohoku-oki earthquake, considering frictional behavior at low to high slip velocities, *Geophys. Res. Lett.*, *38*, L21305, doi:10.1029/2011GL049308.

Simons, M., et al. (2011), The 2011 magnitude 9.0 Tohoku-oki earthquake: Mosaicking the megathrust from seconds to centuries, *Science*, *332*(6036), 1421–1425, doi:10.1126/science.1206731.

Suito, H., T. Nishimura, M. Tobita, T. Imakiire, and S. Ozawa (2011), Interplate fault slip along the japan trench before the occurrence of the 2011 off the Pacific coast of Tohoku earthquake as inferred from GPS data, *Earth Planets Space*, *63*, 615–619.

Uchida, N., and T. Matsuzawa (2011), Coupling coefficient, hierarchical structure, and earthquake cycle for the source area of the 2011 off the Pacific coast of Tohoku earthquake inferred from small repeating earthquake data, *Earth Planets Space*, *63*, 675–679.

Yagi, Y., M. Kikuchi, and T. Nishimura (2003), Co-seismic slip, post-seismic slip, and largest aftershock associated with the 1994 Sanriku-haruka-oki, Japan, earthquake, *Geophys. Res. Lett.*, *30*(22), 2177, doi:10.1029/2003GL018189.

Yamanaka, Y., and M. Kikuchi (2004), Asperity map along the subduction zone in northeastern Japan inferred from regional seismic data, *J. Geophys. Res.*, *109*, B07307, doi:10.1029/2003JB002683.

Zumberge, J. F., M. B. Heflin, D. C. Jefferson, M. M. Watkins, and F. H. Webb (1997), Precise point positioning for the efficient and robust analysis of GPS data from large networks, *J. Geophys. Res.*, *102*(B3), 5005–5017, doi:10.1029/96JB03860.